Available online at www.sciencedirect.com
SCIENCE DIRECT
Biochemical and Biophysical Research Communications 343 (2006) 222–228
BBRC
www.elsevier.com/locate/ybbrc

Investigation of toroidal pore and oligomerization by melittin using transmission electron microscopy

Seong-Cheol Park [a,b], Jin-Young Kim [a], Sun-Oh Shin [a], Chan-Young Jeong [a], Mi-Hyun Kim [a], Song Yub Shin [a,c], Gang-Won Cheong [b,d], Yoonkyung Park [a,e,*], Kyung-Soo Hahm [a,c,*]

[a] *Research Center for Proteineous Materials (RCPM), Chosun University, Kwangju 501-759, Republic of Korea*
[b] *Division of Applied Life Science, Gyeongsang National University, Chinju 660-701, Republic of Korea*
[c] *Department of Medicine, Chosun University, Kwangju 501-759, Republic of Korea*
[d] *Environmental Biotechnology National Core Research Center, Gyeongsang National University, Chinju 660-701, Republic of Korea*
[e] *Department of Biotechnology, Chosun University, Kwangju 501-759, Republic of Korea*

Received 8 February 2006
Available online 24 February 2006

Abstract

We studied the effects of melittin on various cell wall components and vesicles of various lipid compositions. To interact with the cytoplasmic membrane, melittin must traverse the cell wall, which is composed of oligosaccharides. Here, we found that melittin had a strong affinity for chitin, peptidoglycan, and lipopolysaccharide. We further examined the influence of lipid compositions on the lysis of the membranes by melittin. The result showed that melittin bound better to negatively charged than to zwitterionic lipid vesicles but was more potent at inducing leakage from zwitterionic lipid vesicles. Our studies further indicated that the oligomeric state of melittin varied between tetramers and octamers during the formation of toroidal pores. Dextran leakage experiments confirmed the formation and dimension of these toroidal pores. Finally, transmission electron microscopy revealed that melittin formed pores via peptide oligomerization by the toroidal pore-forming mechanism. The toroidal pores composed of 7–8 nm diameter rings that encircled 3.5–4.5 nm diameter cavities on zwitterionic lipid vesicles.

Keywords: Melittin; Oligomerization; Electron microscopy; Toroidal pore

Antimicrobial peptides are known to induce membrane defects such as phase separation, membrane thinning, pore formation, and disruption of bilayer or lamellar lipid structure, depending on the molecular properties of both the lipid and the peptide [1]. A number of models have been proposed to explain how antimicrobial peptides cause membrane permeabilization, including three general models for the interaction of phospholipid membranes and antimicrobial peptides, including the ''barrel-stave'' [2], ''toroidal pore'' [3,4], and ''carpet'' models [5].

Toroidal pore model has been suggested for small antimicrobial peptides such as magainin [3,6] and cathelicidin [7]. This model proposes that the peptides remain associated with the phospholipid headgroup regions of the bilayer, locally inducing a high-curvature fold in the bilayer, so that the two leaflets of the bilayer communicate directly at a torus lined by the peptides. This model differs from the barrel-stave model in that the peptides are always associated with the lipid head groups even when they are perpendicularly inserted in the lipid bilayer [8].

Melittin is the major component of the European honeybee venom (*Apis mellifera*) and is highly cytolytic. This peptide, composed of 26 amino acids, also possesses a broad spectrum of antimicrobial activity and is known to

* Corresponding authors. Fax: +82 62 227 8345.
E-mail addresses: y_k_park@chosun.ac.kr, y_k_park@hanmail.net (Y. Park), kshahm@chosun.ac.kr (K.-S. Hahm).

0006-291X/$ - see front matter © 2006 Elsevier Inc. All rights reserved.
doi:10.1016/j.bbrc.2006.02.090

directly interact with membranes [9,10]. Its structure, determined from crystals grown in aqueous solution, is a bent α-helical rod [11,12]. However, melittin also exists as monomers or tetramers according to the concentration, ionic strength, and pH of the aqueous solution [13,14]. Melittin is considered to be a good model peptide for the development of novel antibiotics due to its ability to disrupt the membrane. To develop novel antibiotics based on melittin, it is essential to determine the molecular mechanism of the melittin–lipid interaction.

The aim of the present study was to investigate the effects of melittin using various lipid compositions and cell wall components and to observe by electron microscopy. The results suggest that melittin forms toroidal pores in zwitterionic lipid vesicles. In addition, we measured the pore size in the zwitterionic vesicles using dextran leakage and transmission electron microscopy.

Materials and methods

Peptide synthesis and purification. Peptides were synthesized using solid phase methods with Fmoc (*N*-(9-fluorenyl)methoxycarbonyl)-protected amino acids on an Applied Biosystems Model 433A peptide synthesizer [15]. 4-Methyl benzhydrylamine resin (Novabiochem) (0.55 mmol/g) was used to produce an amidated C-terminus. For each coupling step, the Fmoc-protected amino acid and coupling reagents were added in 10-fold molar excess with respect to resin concentration. Coupling (60–90 min) was carried out with dicyclohexylcarbodiimide and 1-hydroxy benzotriazole in the presence of *N*-methyl-2-pyrrolidone. Cleavage from the resin and deprotection of the synthesized peptide were carried out with a solution of 90% trifluoroacetic acid, 3% water, 1% triisopropylsilane, and 2% each of 1,2-ethanedithiol, thioanisole, and phenol. After repeated precipitation with ether, the crude peptide was purified using reversed-phase preparative HPLC on a Waters 15 μm Deltapak C18 column (19× 300 mm) using an appropriate 0–60% acetonitrile gradient in 0.1% trifluoroacetic acid. The purity of the purified peptide was checked using analytical reversed-phase HPLC with a Vydac C18 column (4.6× 250 mm, 300 Å, 5 nm).

Peptide binding to microbial cell wall components. To perform in vitro binding assay of melittin, we used Curdlan (β-1,3-glucan; yeast), peptidoglycan (β-1,4-glycosidic linkage between *N*-acetylmuramic acid and *N*-acetylglucosamine; Gram-positive bacteria), chitin (β-1,4-*N*-acetyl-D-glucosamine), and cellulose (β-1,4-glucan). The synthetic peptides were suspended in buffer I (10 mM sodium phosphate, pH 7.4). Insoluble polysaccharides (200 μg) were added to a 200 μl peptide solution (5 μg) and incubated at room temperature with mild agitation for 30 min. The mixtures were centrifuged (12,000*g* for 3 min) and the resulting pellet was washed three times with 0.5 ml of washing buffer (10 mM Tris, pH 7.5, 500 mM NaCl, and 0.02% Tween 20). The peptides bound to the insoluble polysaccharide were detached by adding SDS–PAGE sample buffer and then subjected to 16.5% tricine–SDS–PAGE. The LPS (Gram-negative bacteria) binding assay was carried out in essentially the same method as described above, except that the binding mixture was centrifuged at 22,000*g* for 15 min at each step in order to precipitate small particles of LPS.

Binding of melittin to liposomes. The association between melittin and the change in vesicle size was assessed by visible attenuance measurements. Peptide (5 μM) solutions were added to a suspension of 100 μM SUVs consisting of PC, PE, PG, CH, SM, and PS. Attenuance was measured at 405 nm using a Microplate Autoreader before and after the addition of peptide [16].

To study the binding ability of melittin to LUVs, the sedimentation assay was applied [17,18].

Calcein release from liposomes. The CF leakage of liposomes was measured with a spectrofluorometer (Perkin-Elmer LS55) with peak excitation and emission wavelengths of 480 and 520 nm (band-pass of both beams, 5 nm). The extent of the CF leakage (%) was calculated as follows: Release $(\%) = 100 \times (F - F_0)/(F_t - F_0)$, where F and F_t are the fluorescence intensities before and after the addition of the detergent, respectively, and F_0 represents the fluorescence of intact vesicles [19].

Cross-linking analysis. Melittin was incubated both with and without LUVs for 10 min at room temperature. The samples were then further incubated with 80 μM BS^3 [20] and 0.9 mM DSS [21] for 1 h and 10 min, respectively [22]. After incubation, the samples were added to a tricine sample buffer and subjected to 16.5% tricine–SDS–PAGE without heating. The peptide bands were identified in the gels following Coomassie Brilliant Blue G-250 staining.

Preparation of dextran-loaded liposomes and leakage experiments. FITC-labeled dextran (FD-4, 10, 20, 40, 70, and 500) were utilized as model cytoplasmic component. The leakage of dextran-loaded liposomes was recorded by monitoring the fluorescence intensity of FITC (excitation wavelength: 494 nm, emission wavelength: 520 nm). Hundred percent leakage was achieved upon addition of Triton X-100 to a final concentration of 1 mM. The percent leakage value was plotted [23].

Transmission electron microscopy. Melittin was incubated with SUVs at room temperature in 10 mM sodium phosphate buffer. After incubation, melittin was applied to glow-discharged carbon-coated copper grids. After allowing the peptide and SUVs to absorb for 1 min, the grids were rinsed with the same buffer and stained with 2% (w/v) uranyl acetate. Electron micrographs were then recorded (FEI Technei 12 microscope) at nominal magnifications (×67,000–110,000) and an accelerating voltage of 120 kV.

Electron microscopic examination of bacterial and fungal membranes. Midgrowth phase *Staphylococcus aureus*, *Escherichia coli*, and *Candida albicans* were resuspended at 10^8 CFU/ml in sodium-phosphate buffer, pH 7.4, supplemented with 100 mM NaCl, and incubated at 37 and 28 °C, respectively, with melittin. The cells were fixed with equal volumes of 4% glutaraldehyde and 1% paraformaldehyde in 0.05 M cacodylate buffer (pH 7.2). After fixation for 3 h at 4 °C, the samples were centrifuged at 150*g* and washed twice with 0.05 M cacodylate buffer (pH 7.2). The samples were dehydrated with sequential treatments with 50%, 70%, 90%, 95%, and 100% ethanol. After lyophilization and gold coating, the samples were examined by SEM (HITACHI, Tokyo, Japan).

Results

Recognition of melittin by the cell wall components

To evaluate the specific binding of melittin to microbial cell wall components, we used various insoluble oligosaccharide polymers, including β-1,3-glucan and chitin from yeast, LPS from Gram-negative bacteria, and peptidoglycan from Gram-positive bacteria [24]. As shown in Fig. 1A, melittin bound specifically to chitin, peptidoglycan, and LPS, with greater binding to peptidoglycan and LPS than to chitin. We also compared the in vivo effects of the peptides on *Aspergillus flavus* and *Aspergillus fumigatus*, two fungi that do express chitin, and on *Phytophthora nicotinae* and *Phytophthora parasitica*, two fungi that do not express chitin (data not shown). We found that melittin showed highly potent antimicrobial activity against the chitin-containing fungi but were inactive against the strains that did not contain chitin.

Effects of melittin on membrane binding, disruption, and leakage

We next monitored the effects of melittin on liposomes of varying size and type by measuring the change in liposome turbidity upon the addition of melittin. The turbidity

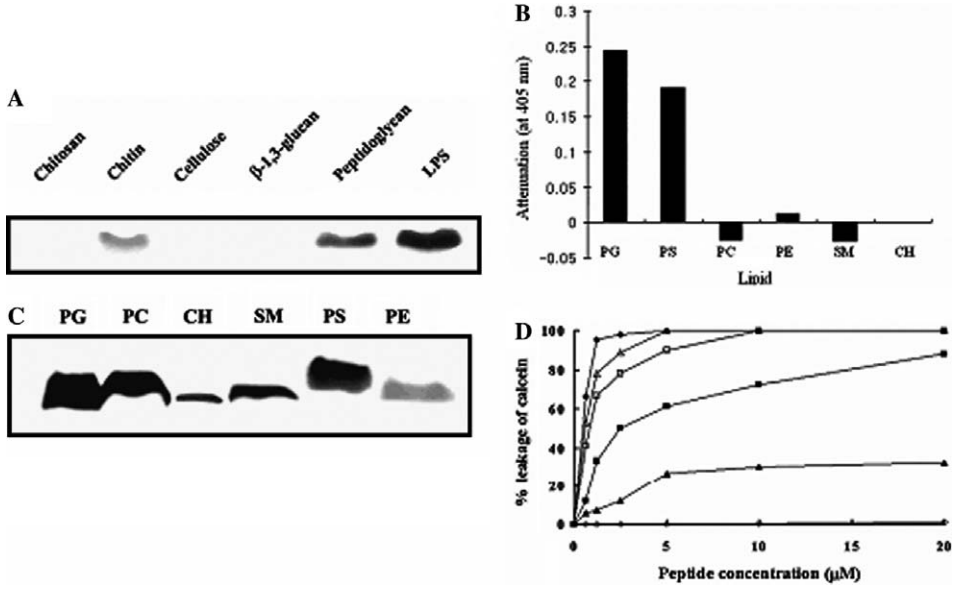

Fig. 1. Interaction of melittin with the cell wall components and lipid vesicles. (A) In vitro binding assay performed using insoluble polysaccharide polymers; (B) with addition of melittin to SUVs, change of turbidity of the mixture was measured. Turbidity is related to vesicle size; (C) melittin, at a concentration of 5 μM, was incubated with 100 μM LUVs. After 30 min incubation, the sample was centrifuged and the pellets were analyzed by SDS–PAGE; (D) melittin-induced dye release from calcein entrapped SUVs. Fluorescence was measured at ~30 min after addition of melittin. Data are presented as a function of peptide concentration for the following SUVs: PC (♦), PG (■), CL (▲), CH (△), SM (□), and PE (◊).

of PG and PS vesicles, which are negatively charged, increased upon the addition of melittin. These results indicate that the size of the vesicle was increased due to lysis and aggregation. In contrast, the turbidity of PC, CH, and SM vesicles decreased and that of PE vesicles did not change (Fig. 1B). We further examined the binding of melittin to liposomes using the method developed by Mileykovskaya et al. [17], which employs SDS–PAGE. Although the degree of binding varied between the different phospholipid vesicles, melittin bound to all of them (Fig. 1C). Binding of melittin was the strongest to negatively charged vesicles. To understand the relationship between binding and permeabilization, we measured the melittin-induced release of calcein entrapped in liposomes composed of various lipids (Fig. 1D). Although melittin bound most strongly to negatively charged vesicles in the binding assay, it was most effective at inducing calcein leakage from zwitterionic liposomes [25].

Oligomeric states of melittin in membranes

To determine the oligomeric state of membrane-bound melittin, we performed chemical cross-linking in the presence of liposomes. As shown in Fig. 2, in PC/CH (1:1, w/w) liposomes, aggregates of tetramers of melittin were observed, whereas, melittin exists as complexes of octamers in PE/PG (1:1, w/w) liposomes.

Determination of the size of the melittin pore

To gain further insight into the pattern and size of melittin-induced membrane defects, we assessed the

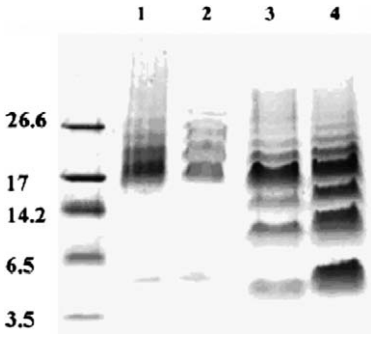

Fig. 2. Oligomeric states on lipid vesicles. Chemical cross-linked samples were prepared as described in Experimental section. (1,2) PC/CH (1:1, w/w) vesicle; (3,4) PE/PG (1:1, w/w) vesicle. First and second lanes of each vesicle indicate system with BS^3 and DSS, respectively.

peptide-induced release of liposome-encapsulated markers of varying size, i.e., FD4 (3.9 kDa, 1.8 nm radius) [26], FD10 (9.9 kDa), FD20 (19.8 kDa, 3.3 nm radius) [25], FD40 (40.5 kDa, 4.8 nm radius) [26], FD70 (71.6 kDa, 5 nm radius) [27], and FD500 (530 kDa) (Fig. 4). In addition, the primary lipid composition of the cytoplasmic membrane surface was mimicked using LUVs composed of PC, 1:1 (w/w) yeast PC/CH, and 1:1 (w/w) bacterial PE/PG. In the PC and PC/CH vesicles, melittin-induced defects allowed the leakage of all of the FD20, but significantly restricted the release of the larger FD40. On the basis of these results, we estimate that melittin forms pores with a cavity radius between 3.3 and 4.8 nm. On the other hand, in PE/PG liposomes, the leakage content did not decrease significantly, making it difficult to estimate the size of the pore (Fig. 3).

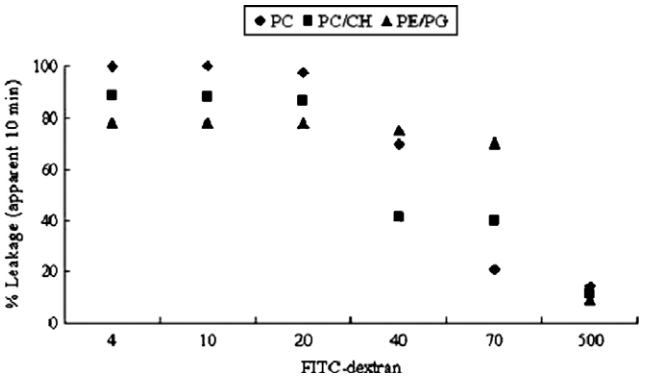

Fig. 3. Determination of pore size on lipid vesicles. Vesicles containing FITC-dextrans of FD4, FD10, FD20, FD40, FD70 or FD500 were incubated in the presence of melittin for 10 min. FITC-dextran release from PC (♦), PC/CH (■), and PE/PG (▲) liposomes.

Melittin oligomers generate ring-like structures

We used transmission electron microscopy to directly examine the structures of the peptide-induced pores. For these experiments, liposomes composed of PC/CH were incubated for 5 min with melittin. The electron micrographs in Fig. 4 show that melittin forms ring-like structures on the vesicles, which can be either attached to the vesicle or be released into the solution (Fig. 4B). The pores consisted of 7–8 nm-wide rings that encircled 3.5–4.5 nm-wide cavities and were formed by the octameric complexes of melittin bound to membrane. The complexes of melittin bound to membrane were shown to oligomeric form, from tetramers and octamers. The results of chemical cross-linking (Fig. 3) and transmission electron microscopy suggest that melittin forms structures ranging from tetramers and octamers.

We also examined the effect of melittin on the morphology of *E. coli*, *S. aureus* and *C. albicans* that was observed using scanning electron microscopy (Fig. 5). When the peptides were applied at concentrations corresponding to 60% MIC, some differences in the morphology of the treated microbial cells were observed. Melittin caused bleb-like structures on over the entire *C. albicans* cell wall (Fig. 5A), whereas *E. coli* and *S. aureus* cells were aggregated (Figs. 5B and C).

Discussion

Most cationic antimicrobial peptides have bacteria cell-selective activity, binding specifically to the negatively charged phospholipids, which are the main components of bacterial cytoplasmic membranes [28,29], and then permeabilizing the membrane. Here, we showed that melittin folds into a helical structure at the membrane and then assembles into oligomers. On the basis of the present results, we propose that, in zwitterionic liposomes, melittin forms a toroidal pore with ring-like structures in zwitterionic. These findings were confirmed directly by transmission electron microscopy, and the results are consistent with previous studies suggesting that melittin forms toroidal pores and that its induction of bilayer leakage depends on the properties of the lipids [8,12].

In most microorganisms, the cytoplasmic membrane is surrounded and supported by a cell wall that provides strength, rigidity, and shape. To interact with the membrane, antimicrobial peptides, including melittin, must pass through the cell wall. Therefore, if they are unable to bind to the cell wall, they may have less or a complete loss of activity. Although this is an important concept, mechanism studies of cell wall components have been reported only for LPS. In this study, we show that melittin can bind to insoluble polysaccharides. In addition, our results indicate that melittin can bind to chitin from yeast, peptidoglycan from Gram-positive bacteria, and LPS from Gram-negative bacteria, which may explain how melittin has such a broad

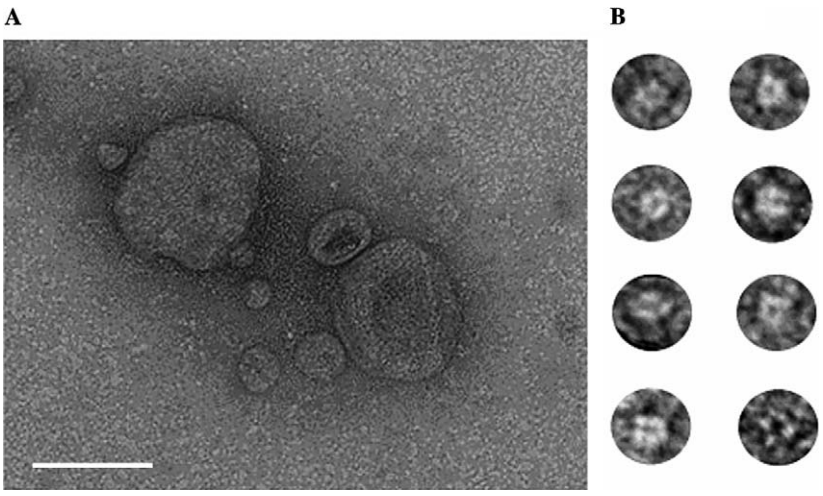

Fig. 4. Electron micrographs show that melittin forms ring-like structures on PC/CH liposomes. (A) Electron micrograph of PC/CH liposome incubated with 5 μM of melittin for 1 min. Scale bars, 100 nm. (B) The galleries of ring-shaped molecules, which are either attached to a liposome or released.

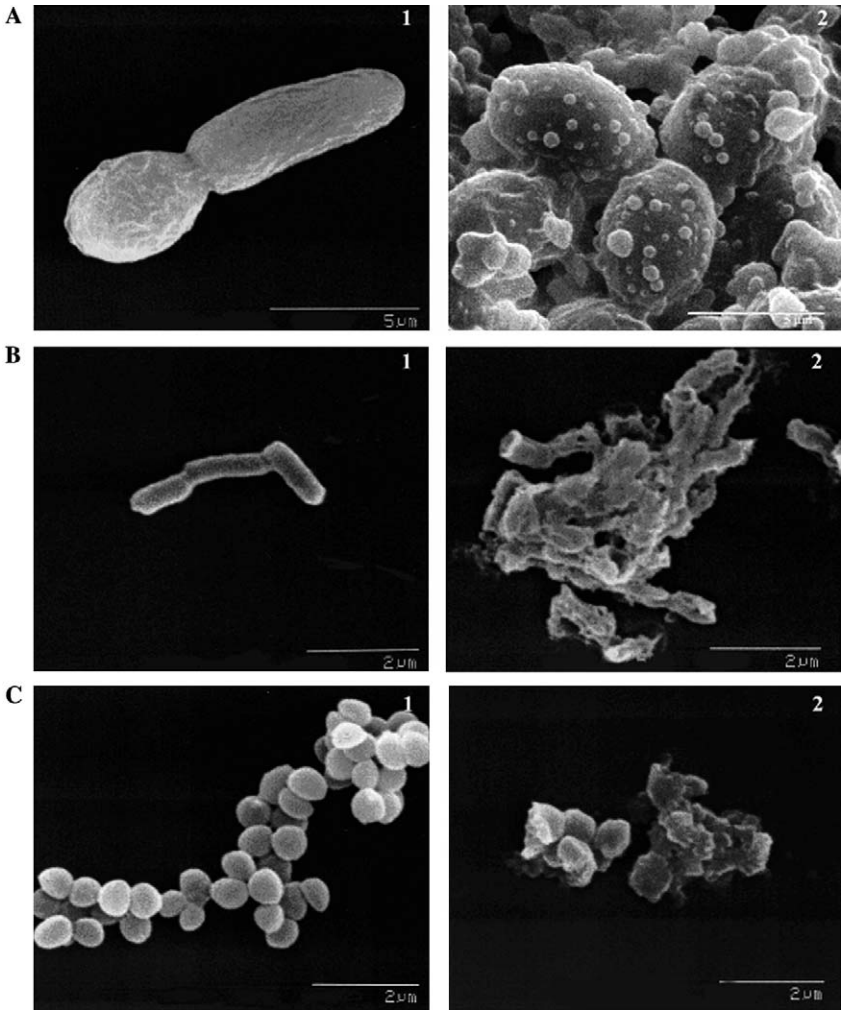

Fig. 5. Morphological changes in intact cells. *Candida albicans* (A), *Escherichia coli* (B), *Staphylococcus aureus*, and (C) were treated with melittin at their MICs. (1) Untreated cells and (2) treated cells.

antimicrobial activity (Fig. 1A). The high negative charge of LPS may explain why it strongly binds melittin. Although LPS can serve as a physical barrier to cytoplasmic membrane targets [30,31], we suspect that it assists in the rapid initial recognition of melittin [32] and its folding into a helical structure. This interaction alone, of course, does not completely explain its broad antimicrobial activity.

To clarify how melittin interacts with various lipids, we analyzed the change of liposome size, mean ellipticity, and binding of melittin in liposomes with different lipid composition. Our results suggest that melittin is induced to helical form in lipids, the effect was stronger in negatively charged vesicles than in zwitterionic vesicles. This may be due to a strong electrostatic interaction between negatively charged lipids and melittin. We also found that melittin binds to all lipids, although to different extents. This indicates that the charge and hydrophobicity of melittin are essential for its interaction with membranes (Fig. 1C).

Our chemical cross-linking experiments suggested that melittin existed as tetramers to octamers (Fig. 2). Magainin also induces the formation of toroidal pores, and they have a more variable pore size than alamethicin-induced pores, which form barrel-stave pores. Similar to the melittin pores, they have an inner diameter of 3–5 nm and an outer diameter of 7–8.4 nm. In this case, each pore appears to be made up of only 4–7 magainin monomers and approximately 90 lipid molecules [11].

The FITC-dextran leakage suggested the formation of toroidal pores with an internal diameter of 3.3–4.8 nm (Fig. 3). Our data also are consistent with previously reported vesicle leakage experiments indicating pore sizes up to approximately 3 nm in diameter, with the pore size increasing as the melittin concentration was raised. Moreover, neutron diffraction studies by Yang et al. [33] suggested that the internal and external diameters of the melittin pores are 4.2 and 7.7 nm, respectively.

We also investigated the effect of a short incubation with a high concentration of melittin on the ultrastructure of the toroidal pore. Fortunately, under these conditions, there was minimal destruction of liposomes, and we were able to detect ring-like structures on the surface of the vesicle by transmission electron microscopy (Fig. 4). The detailed

features of these ring-like structures could be more readily observed in the high-magnification images. Interestingly, these images revealed that these rings released from the liposomes, suggesting that melittin generates pores via the formation of micelles, which eventually leads to liposome destruction. On the basis of our results, we suggest that melittin can form toroidal pores with a diameter of 7–8 nm surrounding a central cavity with diameter of 3.5–4.5 nm.

Fig. 6 depicts a model to explain how melittin disrupts zwitterionic lipid vesicles, which mimic fungal membranes. In this scheme, the lipids induce the formation of amphiphilic helix structures in melittin. Once inserted in the membrane, the melittin aggregates, causing the lipids to bend, which results in the formation of toroidal pores and the subsequent leakage of cytosolic material. During the formation of the toroidal pore, the polar faces of melittin bind initially to the polar head groups of the lipid, after which the hydrophobic faces of melittin tilt to the hydrophobic cores because the strength of association is stronger than those of the polar regions and because the hydrophobic face of melittin repels water. At this point, melittin may begin to self-associate. Continuous bending in the two leaflets of the membrane induces the toroidal hole, which is a membrane-spanning pore lined with the polar faces of melittin and the polar headgroups of the lipid. As a result, adjacent faces of melittin molecules do not aggregate. With time, unattached melittin binds to free regions in vesicles, and at a critical concentration and time, the bilayer curvature is disrupted and the membrane disintegrates into micelles. Once the lipids are in micelles, they are unable to aggregate. This hypothesis relies on the formation of soluble melittin–lipid micelles. Moreover, the following experiments were performed to evaluate a difference between zwitterionic and anionic membrane. We found that equimolar amounts of melittin caused negatively charged membranes to aggregate and fuse (data not shown).

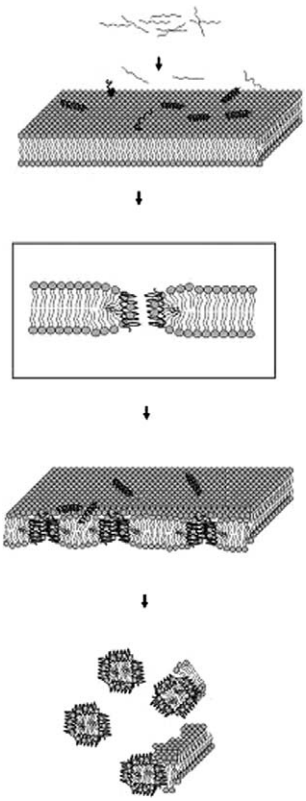

Fig. 6. Schematic diagram illustrating the interactions of melittin with the bacterial cytoplasmic membrane. The peptides reach the outer bacterial membrane as oligomers, bind to the surface, and induce pore formation in the cytoplasmic membrane via the toroidal model. In this model, the attached peptides aggregate and induce the lipid monolayers to bend continuously through the pore so that the channel is lined by both the inserted peptides and the lipid head groups.

In conclusion, the effect of melittin on various artificial liposomes forms toroidal pores that progress to micelles, where its effects are mostly due to hydrophobic or electrostatic interactions.

Acknowledgments

This work was supported by a grant from the Ministry of Science and Technology, Korea, and the Korea Science and Engineering Foundation through the Research Center for Proteineous Materials (R11-2000-083-00000-0) and from Chosun University, 2005. And S-C Park is supported by scholarships from the BK21 Program, Ministry of Education and Human Resources Development, Korea.

References

[1] E. Habermann, Bee and wasp venoms, Science 177 (1972) 314–322.
[2] K. He, S.J. Ludtke, D.L. Worcester, H.W. Huang, Neutron scattering in the plane of membranes: structure of alamethicin pores, Biophys. J. 70 (1996) 2659–2666.
[3] L. Yang, T.A. Harroun, T.M. Weiss, L. Ding, H.W. Huang, Barrel-stave model or toroidal model? A case study on melittin pores, Biophys. J. 81 (2001) 1475–1485.
[4] I. Zelezetsky, S. Pacor, U. Pag, N. Papo, Y. Shai, H.G. Sahl, A. Tossi, Controlled alteration of the shape and conformational stability of α-helical cell-lytic peptides: effect on mode of action and cell specificity, Biochem. J. 390 (2005) 177–188.
[5] C.E. Dempsey, The actions of melittin on membranes, Biochim. Biophys. Acta 1031 (1990) 143–161.
[6] A.S. Ladokhin, S.H. White, 'Detergent-like' permeabilization of anionic lipid vesicles by melittin, Biochim. Biophys. Acta 1514 (2001) 253–260.
[7] H. Vogel, F. Jahnig, The structure of melittin in membrane, Biophys. J. 50 (1986) 573–582.
[8] T.C. Terwilliger, D. Eisenberg, The structure of melittin. I. Structure determination and partial refinement, J. Biol. Chem. 257 (1982) 6010–6015.
[9] Z. Oren, Y. Shai, Mode of action of linear amphipathic α-helical antimicrobial peptides, Biopolymers 47 (1998) 451–463.
[10] S. Ohki, E. Marcus, D.K. Sukumaran, K. Arnold, Interaction of melittin with lipid membranes, Biochim. Biophys. Acta 1194 (1994) 223–232.
[11] K. Matsuzaki, K. Sugishita, N. Ishibe, M. Ueha, S. Nakata, K. Miyajima, R.M. Epand, Relationship of membrane curvature to the formation of pores by magainin 2, Biochemistry 37 (1998) 11856–11863.
[12] G. Basanez, A.E. Shinnar, J. Zimmerberg, Interaction of hagfish cathelicidin antimicrobial peptides with model lipid membranes, FEBS Lett. 532 (2002) 115–120.

[13] M. Iwadate, T. Asakura, M.P. Williamson, The structure of the melittin tetramer at different temperatures an NOE-based calculation with chemical shift refinement, Eur. J. Biochem. 257 (1998) 479–487.
[14] D. Allende, S.A. Simon, T.J. McIntosh, Melittin-induced bilayer leakage depends on lipid material properties: evidence for toroidal pores, Biophys. J. 88 (2005) 1828–1837.
[15] B. Merrifield, Solid phase synthesis, Science 232 (1986) 341–347.
[16] M. Motizuki, T. Itoh, T. Satoh, S. Yokota, M. Yamada, S. Shimamura, T. Samejima, K. Tsurugi, Lipid-binding and antimicrobial properties of synthetic peptides of bovine apolipoprotein A-II, Biochem. J. 342 (1999) 215–221.
[17] E. Mileykovskaya, I. Fishov, X. Fu, B.D. Corbin, W. Margolin, W. Dowhan, Effects of phospholipid composition on MinD–membrane interactions in vitro and in vivo, J. Biol. Chem. 278 (2003) 22193.
[18] Z. Hu, E.P. Gogol, J. Lutkenhaus, Dynamic assembly of MinD on phospholipid vesicles regulated by ATP and MinE, Proc. Natl. Acad. Sci. USA 99 (2002) 6761–6766.
[19] K. Matsuzaki, K. Sugishita, K. Miyajima, Interactions of an antimicrobial peptide, magainin 2, with lipopolysaccharide-containing liposomes as a model for outer membranes of Gram-negative bacteria, FEBS Lett. 449 (1999) 221–224.
[20] M. Onaderra, J.M. Mancheno, J. Lacadena, V. de los Rios, A. Martinez del Pozo, J.G. Gavilanes, Oligomerization of the cytotoxin α-sarcin associated with phospholipid membranes, Mol. Membr. Biol. 15 (1998) 141–144.
[21] M. Edgerton, S.E. Koshlukova, T.E. Lo, B.G. Chrzan, R.M. Straubinger, P.A. Raj, Candidacidal activity of salivary histatins. Identification of a histatin 5-binding protein on *Candida albicans*, J. Biol. Chem. 273 (1998) 20438–20447.
[22] J.V. Staros, *N*-Hydroxysulfosuccinimide active esters: bis(*N*-hydroxysulfosuccinimide) esters of two dicarboxylic acids are hydrophilic, membrane-impermeant, protein cross-linkers, Biochemistry 21 (1982) 3950–3955.
[23] O.S. Belokoneva, H. Satake, E.L. Mal'tseva, N.P. Pal'mina, E. Villegas, T. Nakajima, G. Corzo, Pore formation of phospholipid membranes by the action of two hemolytic arachnid peptides of different size, Biochim. Biophys. Acta 1664 (2004) 182–188.
[24] Y.S. Kim, J.H. Ryu, S.J. Han, K.H. Choi, K.B. Nam, I.H. Jang, B. Lemaitre, P.T. Brey, W.J. Lee, Gram-negative bacteria-binding protein, a pattern recognition receptor for lipopolysaccharide and β-1,3-glucan that mediates the signaling for the induction of innate immune genes in *Drosophila melanogaster* cells, J. Biol. Chem. 275 (2000) 32721–32727.
[25] A.A. Sobko, E.A. Kotova, Y.N. Antonenko, S.D. Zakharov, W.A. Cramer, Effect of lipids with different spontaneous curvature on the channel activity of colicin E1: evidence in favor of a toroidal pore, FEBS Lett. 576 (2004) 205–210.
[26] M.P. Bohrer, W.M. Deen, C.R. Robertson, J.L. Troy, B.M. Brenner, Influence of molecular configuration on the passage of macromolecules across the glomerular capillary wall, J. Gen. Physiol. 74 (1979) 583–593.
[27] T.C. Laurent, K.A. Granath, Fractionation of dextran and Ficoll by chromatography on Sephadex G-200, Biochim. Biophys. Acta 136 (1967) 191–198.
[28] Y. Shai, From innate immunity to de novo designed antimicrobial peptides, Curr. Pharm. Des. 8 (2002) 715–725.
[29] R.E. Hancock, A. Rozek, Role of membranes in the activities of antimicrobial cationic peptides, FEMS Microbiol. Lett. 206 (2002) 143–149.
[30] D. Allende, T.J. McIntosh, Lipopolysaccharides in bacterial membranes act like cholesterol in eukaryotic plasma membranes in providing protection against melittin-induced bilayer lysis, Biochemistry 42 (2003) 1101–1108.
[31] N. Papo, Y. Shai, A molecular mechanism for lipopolysaccharide protection of Gram-negative bacteria from antimicrobial peptides, J. Biol. Chem. 280 (2005) 10378–10387.
[32] P. Li, T. Wohland, B. Ho, J.L. Ding, Perturbation of lipopolysaccharide (LPS) micelles by Sushi 3 (S3) antimicrobial peptide. The importance of an intermolecular disulfide bond in S3 dimer for binding, disruption, and neutralization of LPS, J. Biol. Chem. 279 (2004) 50150–50156.
[33] L. Yang, T.A. Harroun, T.M. Weiss, L. Ding, H.W. Huang, Barrel-stave model or toroidal model? A case study on melittin pores, Biophys. J. 81 (2001) 1475–1485.